SATELLITE SAR OBSERVATION OF SOLITARY INTERNAL WAVE OCCURRENCE IN THE NORTHERN SOUTH CHINA SEA

Quanan Zheng[1], R. Dwi Susanto[2], Chung-Ru Ho[3], Y. Tony Song[4], and Qing Xu[1]

[1]Department of Atmospheric and Oceanic Science, University of Maryland, College Park, Maryland, USA
quanan@atmos.umd.edu
[2]Lamont-Doherty Earth Observatory of Columbia University, Palisades, New York, USA
dwi@ldeo.columbia.edu
[3]Department of Marine Environmental Informatics, National Taiwan Ocean University, Keelung, Taiwan
chungru@sun4.oce.ntou.edu.tw
[4]Jet Propulsion Laboratory, California Institute of Technology, Pasadena, California, USA
song@pacific.jpl.nasa.gov

ABSTRACT Satellite synthetic aperture radar (SAR) images from 1995 to 2001 and field measurements of sea surface wind, sea state, and vertical stratification are used for statistical analyses of internal wave (IW) occurrence and SAR imaging conditions in the northern South China Sea (NSCS). Latitudinal distribution of IW packets shows that 22% of IW packets distributed in the east of 118°E and 78% of IW packets in the west of 118°E. The yearly distribution of IW occurrence frequencies reveals an interannual variability. The monthly SAR-observed IW occurrence frequencies show that the high frequencies are distributed from April to July and reach a peak in June. The low occurrence frequencies are distributed in winter from December to February of next year. These statistical features are explained by solitary wave dynamics.

KEYWORDS: ocean internal waves, solitary waves, South China Sea, satellite SAR image.

1. INTRODUCTION

The northern South China Sea is an ocean area where the energetic internal waves occur frequently [Hsu and Liu, 2000; Liu et al., 2004]. Liu et al. [1998] suggested that the IWs might be generated by localized boundary conditions. Ebbesmeyer et al. [1991] suggested that the IWs near the Luzon Strait might be generated by tidal current passing through the channels between islands or sills. Yuan et al. [2006] proved that the IWs can be induced by the instability of the Kuroshio. All the hypotheses must face to a challenge, i.e., how to explain the interannual and seasonal variability of IW occurrence, as well as asymmetric distribution of IW packets to the submarine ridges? The motivation of this study is to look for dynamical mechanisms best suitable for description of solitary wave behavior, and giving proper explanations to the seasonal variability of IW generation.

2. STATISTICS OF IW OCCURRENCE

2.1 Satellite SAR data

Seven years of SAR images taken by ERS-1/2 (European Remote Sensing satellites) from 1995 to 2001 are used for the statistical analysis. Figure 1 shows an example of satellite SAR images. The imaged area is 528 km by 478 km centered at 21°09' N latitude 116°18' E longitude. Grouped bright lines distributed in the central portion are imagery of westward-propagating IW packets.

Figure 1. A RADARSAT ScanSAR image of NSCS taken on April 26, 1998.

2.2 Latitudinal distribution

A map of the study area with crest lines of leading waves in IW packets is shown in Figure 2. One can see that almost all IW packets are concentrated within a latitudinal band from 20° to 22°N. All IW packets show the same westward propagation direction. On the east side, the IW packet distribution area is defined by the submarine ridges extending from the southern tip of Taiwan Island all the way crossing the Luzon Strait.

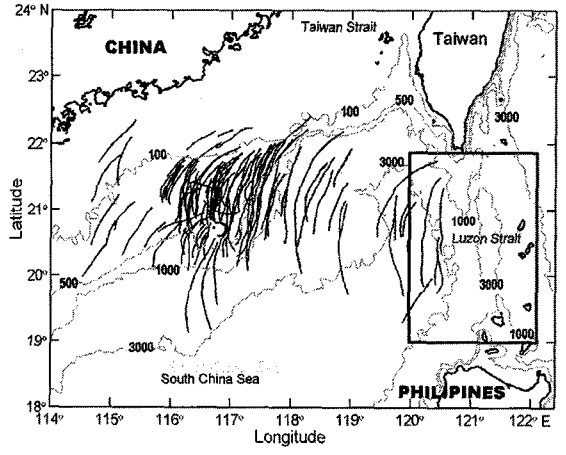

Figure 2. A map of the study area. Bold lines represent crest lines of leading waves in IW packets interpreted from SAR images. The rectangular box on the right defines an IW generation source region .

One can see that the bottom topography in the source region is generally symmetric about the underwater ridges. The tidal currents are always reciprocal anywhere. Thus, the IW packets should be generated symmetrically on both sides of the topography if the tide-topography generation stands as a sole mechanism. But, in Figure 2, no IW packet is found on the east side of the ridges.

2.3 Yearly IW occurrence frequency

The SAR-observed IW occurrence frequency defined as

$$p_i = q_i \left(N_i \Big/ \sum_j N_j \right), \qquad (1)$$

where N_i (N_j) is a number of days on which the IW is imaged by SAR, here $i(j)$ represents the i-th (j-th) year, $q_i = D_{1997}/ D_i$ as a yearly de-weighted factor, here D_{1997} is a number of SAR working days over the study area in 1997, and D_i is the SAR working days in the i-th year. The statistical results are shown in Figure 3. One can see an obvious interannual variability of SAR-observed IW occurrence frequency in NSCS. In 1995, 1998, and 2000, the frequencies are 2 to 4 times higher than that in other years. This interannual variability implies that there are long-term and large scale processes playing roles in modifying IW occurrence frequency and SAR imaging in NSCS.

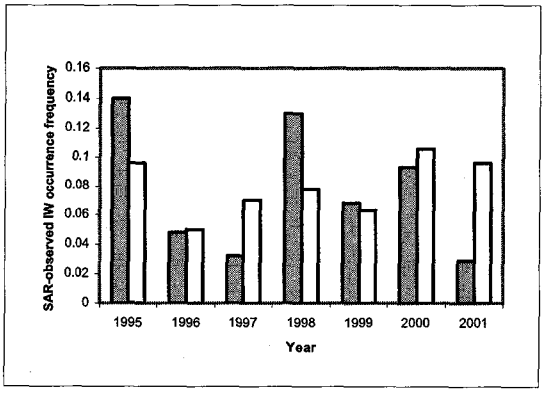

Figure 3. Yearly distribution of SAR-observed IW occurrence frequencies in NSCS calculated by this study (dark bars) and in Meng [2002] (open bars).

2.4 Monthly IW occurrence frequency

The monthly SAR-observed IW occurrence frequency is defined as

$$p_{mi} = q_{mi} \left(n_i \Big/ \sum_{j=1}^{12} n_j \right), \qquad (2)$$

where n_i (n_j) is a number of total days in the i-th (j-th) month of seven years, at which the IWs were imaged, and $q_{mi} = d_8 / d_i$ as a monthly de-weighted factor, here d_8 is a minimum number of SAR working days over the study area in August, and d_i is the SAR working days in the i-th month. The calculation results are shown in Figure 4.

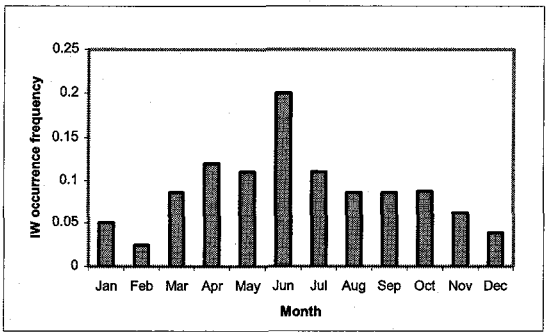

Figure 4. Monthly distribution of SAR-observed IW occurrence frequencies in NSCS de-weighted by low sea states.

3. DYNAMICAL ANALYSIS

All IW theories have verified that the vertical stratification is a decisive factor for IW propagation [Zheng et al., 2001a; 2001b]. This study proposes that the solitary internal waves are generated in a source region. Working like an oscillator, the source region has the potential to provide the necessary and sufficient conditions for wave generation: 1) initial disturbance formation, and 2) wave amplitude growth. The source region also dissipates the disturbance energy, so that only fully developed waves are able to radiate out of the source region.

3.1 Physical model and scale analysis

A typical case of shoaling thermocline and IW packet observed in the source region is shown in Figure 5. Physically, the internal soliton growth problem is equivalent to the evolution problem of surface soliton propagating along a shoaling beach. The soliton amplitude satisfies the perturbed KdV equation [Newell, 1985]

$$q_\tau + 6qq_\theta + q_{\theta\theta\theta} = -\frac{9}{4}\frac{D_\tau}{D}q, \qquad (3)$$

where τ is a rescaled distance coordinate

$$\tau = \frac{1}{6}\int^X D^{1/2}dX, \qquad (4)$$

θ is the retarded time

$$\theta = -t + \frac{1}{\varepsilon}\int^X \frac{dX}{D^{1/2}}, \qquad (5)$$

where t is the time, D is the nondimensional depth of the upper layer, $D = 1 + h$, in which $h = H(x)/h_0$, $X = \varepsilon x$, and the subscript represents partial differential with respect to that variable.

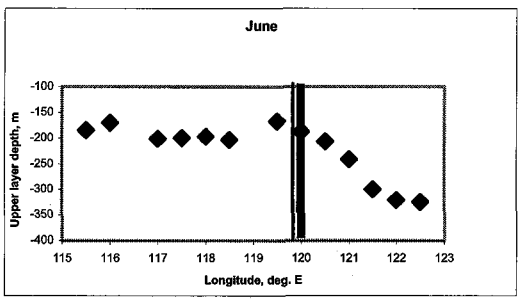

Figure 5. Monthly mean upper layer depth of June in NSCS. Double bars represent the location of IW packet.

3.2 Soliton amplitude growth ratio

From the theoretical model, the soliton amplitude growth ratio (SAGR) is calculated by

$$SAGR = (h_0/d)^{3/2}, \qquad (15)$$

where h_0 and d are the upper layer depths on the deep side and shallow side of the shoaling thermocline defined by 15°C isotherm. The results are shown in Figure 6.

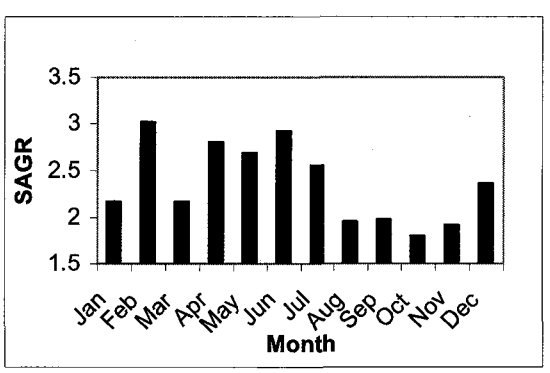

Figure 6. Monthly mean SAGR in the Luzon Strait derived from the temperature profile data.

The monthly SAR-observed IW occurrence frequency versus the monthly mean SAGR (except winter months) derived from upper layer depths is plotted in Figure 7. One can see that the theoretical model gives a trend of data points with a correlation coefficient (R^2) of 0.6519.

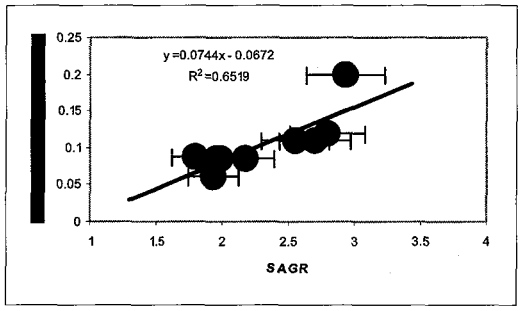

Figure 7. The monthly IW occurrence frequency versus the monthly mean SAGR in NSCS. The error bars represent a maximum error of 10%.

4. CONCLUSIONS

This study proposes that the IW generation needs the necessary and sufficient conditions: initial disturbance formation and wave amplitude growth. The tides, tide-topography interaction, and west boundary current instability are treated as the necessary conditions for initial disturbance formation, but not the sufficient conditions for IW generation. Due to dissipation of the initial disturbance, only fully developed waves have a chance to radiate out of the source region. From the physical model, PKdV equation, and solvability conditions, the sufficient conditions for solitary IW growth are derived. The results indicate that the thermocline shoaling provides the forcing to the amplitude growth for westward propagating disturbances, so that the soliton amplitude growth ratio is a key factor for the variation of the IW occurrence frequency. The eastward propagating initial disturbances have no chance to grow up, therefore, they are hardly observed on the east side of submarine ridges in the eastern Luzon Strait.

References

Boyer, T., and S. Levites, 1994. Quality control and processing of historical oceanographic temperature, salinity, and oxygen data, *NOAA Technical Report NESDIS 81*, Washington, D.C., pp. 1-64.

Ebbesmeyer, C. C., C. A. Coomes, and R. C. Hamilton, 1991. New observation on internal wave (soliton) in the South China Sea using acoustic Doppler current profiler, in *Marine Technology Society Proceedings*, New Orleans, pp. 165-175.

Hsu, M.-K., and A. K. Liu, 2000. Nonlinear internal waves in the South China Sea, *Canadian J. Rem. Sens.*, 26, 72-81.

Liu, A. K., Y. S. Chang, M.- K. Hsu, and N. K. Liang, 1998. Evolution of nonlinear internal waves in the East and South China Seas, *J. Geophys. Res.*, 103, 7995-8008.

Liu, A. K., S. R. Ramp, Y. Zhao, and T. Y. Tang, 2004. A case study of internal solitary wave propagation during ASIAEX 2001, *IEEE J. Ocean. Eng.*, 29, 1144-1156.

Meng, J., 2002. *A study of information extraction technology of ocean internal waves from SAR images*, Ph. D. Dissertation, Ocean University of Qingdao, China, pp. 1-114.

Newell, A. C., 1985. *Soliton in Mathematics and Physics*, Society for Industrial and Applied Mathematics, Philadelphia, pp. 1-246.

Yuan, Y., Q. Zheng, D. Dai, X. Hu, F. Qiao, and J. Meng, 2006. The mechanism of internal waves in the Luzon Strait, *J. Geophys. Res.*, in press.

Zheng, Q., Y. Yuan, V. Klemas, and X.-H. Yan, 2001a. Theoretical expression for an ocean internal soliton SAR image and determination of the soliton characteristic half width, *J. Geophys. Res.*, 106, 31,415-31,423.

Zheng, Q., V. Klemas, X.-H. Yan, and J. Pan, 2001b. Nonlinear evolution of ocean internal solitons as propagating along inhomogeneous thermocline, *J. Geophys. Res.*, 106, 14,083-14,094.

Acknowledgements. This work was supported by ONR through grants N00014-05-1-0328, N00014-05-1-0606, N00014-04-1-0698, and N00014-05-1-0272, and partially by NASA JPL through subcontract NMO710968. ERS-1/2 images are copyrighted by ESA.